

# High Performance Polymer Composites on PEEK Reinforced with Aluminum Oxide

R. K. Goyal,<sup>1</sup> Y. S. Negi,<sup>1\*</sup> A. N. Tiwari<sup>2</sup>

<sup>1</sup>Polymer and Materials R&D, Center for Materials for Electronics Technology, Department of Information Technology, Govt. of India, Pune 411008, India

<sup>2</sup>Department of Metallurgical Engineering and Materials Science, Indian Institute of Technology, Mumbai 400 076, India

Received 13 May 2005; accepted 1 September 2005

DOI 10.1002/app.23083

Published online in Wiley InterScience (www.interscience.wiley.com).

**ABSTRACT:** A study on high performance poly(ether-ether-ketone) (PEEK) composites prepared by incorporating aluminum oxide ( $\text{Al}_2\text{O}_3$ ), 0 to 50 wt % by hot compaction at 15 MPa and 350°C was described. Density, thermogravimetric analysis/differential scanning calorimetry, and scanning electron microscopy (SEM) were employed to evaluate their density, thermal stability, crystallinity, and morphology. Experimental density was found higher than theoretical density, which indicates that composite samples are sound. It was found that the addition of micron sized ( $< 15 \mu\text{m}$ )  $\text{Al}_2\text{O}_3$  increased the peak crystallization temperature by 12°C when compared with neat PEEK with insignificant increase in melting temperature. Half-time of crystallization

is reduced from 2.05 min for the neat PEEK to 1.08 min for PEEK incorporated with 30 wt %  $\text{Al}_2\text{O}_3$  because of the strong nucleation effect of  $\text{Al}_2\text{O}_3$ . The thermal stability of composites in air atmosphere was increased by 26°C. However, thermal stability in nitrogen atmosphere decreases at lower concentration of  $\text{Al}_2\text{O}_3$  but increases above 20 wt % of  $\text{Al}_2\text{O}_3$ . Uniform dispersion of  $\text{Al}_2\text{O}_3$  particles was observed in PEEK polymer matrix by SEM. © 2006 Wiley Periodicals, Inc. *J Appl Polym Sci* 100: 4623–4631, 2006

**Key words:** PEEK; aluminum oxide; composites; density; crystallization

## INTRODUCTION

High performance polymer composites reinforced with ceramic particles such as  $\text{Al}_2\text{O}_3$ , AlN, BN,  $\text{Si}_3\text{N}_4$ , SiC,  $\text{SiO}_2$ , and others result in unique combination of properties, which make them useful in aerospace structures, electronics/microelectronics substrates, automotive parts, marine structures, and biomedical applications. By introducing reinforcing particles or fibers in polymers, composite properties can be tailored to meet specific design requirements such as low density, high strength, high stiffness, high damping, chemical resistance, thermal shock resistance, high thermal conductivity, low coefficient of thermal expansion, and good electrical properties.

The properties of particulate composites are strongly dependent on particle shape, particle size, particle distribution, particle loading, type of matrix, and interface between particle and matrix.<sup>1–6</sup> The addition of inorganic fillers or particles to a

polymer has been a common practice to improve the mechanical properties. Among inorganic fillers, calcium carbonate has been one of the most commonly used fillers for commodity plastics such as HDPE<sup>6</sup> and polypropylene (PP),<sup>7</sup> to reduce the cost of the expensive resins. It would be worth noting that these additions also incur a performance cost. Speciality polymers such as poly(ether-ether-ketone) (PEEK), Polyimides, PTFE, LCPs, PPS, PES, etc. with good thermal stability and mechanical properties are required for the applications where performance is more important than cost.

Poly(oxy-1,4-phenyleneoxy-1,4-phenylenecarbonyl-1,4-phenylene) more commonly known as poly(ether-ether-ketone) (PEEK) is a high performance aromatic thermoplastic semicrystalline polymer. PEEK exhibits glass-rubber ( $\infty$ ) or glass-transition temperature ( $T_g$ ) at 143°C and increases as much as 20°C with the degree of crystallinity of the polymer because of the relative constraint imposed on the amorphous phase motions by the crystallinity.<sup>8,9</sup> By using dielectric spectroscopy, Huo et al. reported that amorphous PEEK showed glass transition at 164°C because of mobile amorphous phase relaxation followed by additional relaxation at 195°C (at 1 MHz) because of rigid amorphous phase relaxation. It was also reported that dielectric  $T_g$  is always about 20°C higher than the differential scanning calorimetric  $T_g$ .<sup>9,10</sup> The

Correspondence to: Y. S. Negi (dr\_yuvrjas\_negi@yahoo.co.in).

\*Present address: Polymer Science and Technology Laboratory, Department of Paper Technology, Indian Institute of Technology, Roorkee (IITR), Saharanpur Campus, Saharanpur-247 001, Uttar Pradesh, India.

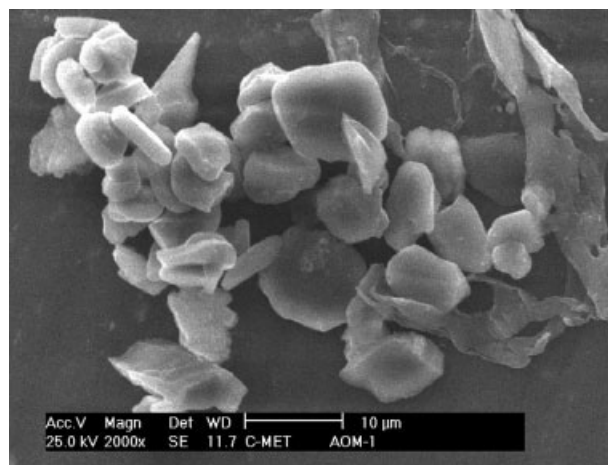
subglass  $\beta$  and  $\gamma$  relaxations observed by dynamic mechanical analyzer or dielectric spectroscopy occurs about  $-63^{\circ}\text{C}$ , and  $-143^{\circ}\text{C}$ , respectively. The  $\beta$  relaxation is affected by the presence of water content, ageing history and crystallinity. The highly localized  $\gamma$  relaxation resulting due to wagging of the polar bridges is insensitive to ageing history, and crystallinity.<sup>11,12</sup>

The double melting behavior, low-temperature melting endotherm, and high-temperature melting endotherm ( $\sim 335^{\circ}\text{C}$ ) of PEEK has been investigated extensively by differential scanning calorimetry.<sup>13,14</sup> The lower melting endotherm peak shifted toward the higher temperature with increasing either the crystallization temperature or the annealing time, while the higher melting endotherm peak remains unchanged.<sup>13</sup> However, these peaks also depend linearly on the logarithm of the differential scanning calorimetry (DSC) heating rate. The two melting endotherms coalesce into one at high heating rates.<sup>14</sup>

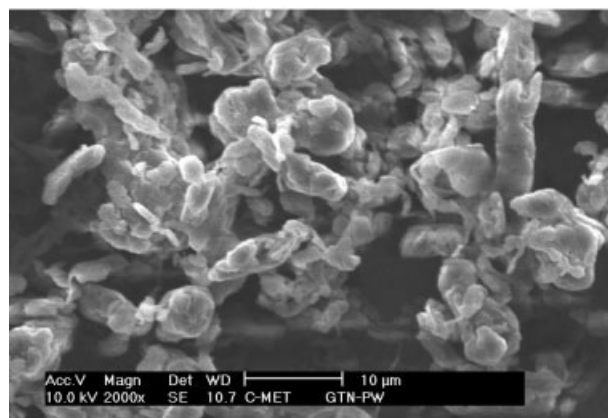
PEEK exhibits outstanding resistance to moisture, chemical and hard radiation, high-temperature thermal stability, impact resistance and wear resistance, and high continuous service temperature up to  $250^{\circ}\text{C}$ , as a result the polymer is used in high temperature engineering applications,<sup>15-17</sup> aerospace,<sup>1</sup> automotive, structural,<sup>1</sup> tribology,<sup>18-21</sup> and biomedical applications.<sup>22</sup>

There are a several hundred publications on the effect of ceramic particles on different polymer properties, but there is rare literature on the effect of  $\text{Al}_2\text{O}_3$  on PEEK. However, recently Kuo et al. have studied the effect of nano- $\text{Al}_2\text{O}_3$  and nano- $\text{SiO}_2$  on PEEK's mechanical and thermal properties.<sup>23</sup> Hydroxyapatite (HA) reinforced PEEK has been reported as biomedical material.<sup>22</sup> Wang et al. have reported the wear and friction properties of PEEK reinforced with various weight fractions of  $\text{SiC}$ ,  $\text{SiO}_2$ ,  $\text{Si}_3\text{N}_4$ , and  $\text{ZrO}_2$ .<sup>18-21</sup> The melting, crystallization, and thermal stability behavior of micron size  $\text{Al}_2\text{O}_3$ -reinforced PEEK was not discussed so far. Sandler et al. have studied the thermal and mechanical properties of carbon nanofibers-reinforced PEEK nanocomposites.<sup>24</sup>

In the present article, a systematic investigation of the  $\text{Al}_2\text{O}_3$ /PEEK composites prepared by mixing PEEK and  $\text{Al}_2\text{O}_3$  in alcohol medium followed by hot pressing technique was reported. The density, thermal stability, melting, and crystallization temperature of the composites were characterized by using density, thermogravimetric analysis (TGA), DSC, respectively. The dispersion of the  $\text{Al}_2\text{O}_3$  particles was observed by scanning electron microscopy (SEM). The thermomechanical and electrical properties of the composites will be presented elsewhere.



(a)



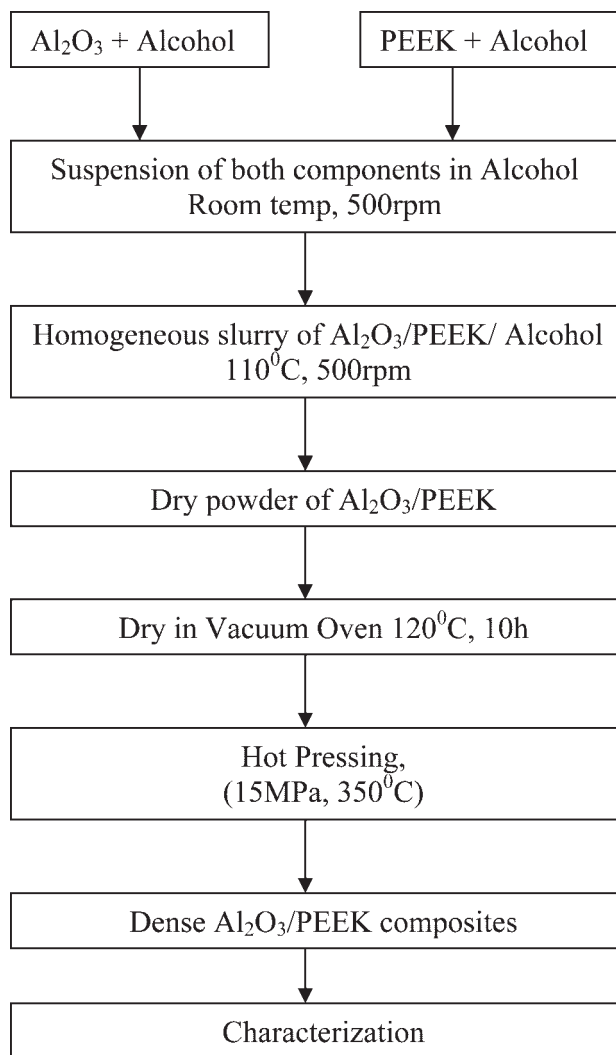
(b)

**Figure 1** SEM micrographs of (a) aluminum oxide (b) PEEK powder.

## EXPERIMENTAL

### Materials

The commercial PEEK, grade 5300PF donated by Gharda Chemicals Ltd. Panoli, Gujarat, India, under the trade name GATONE™ PEEK was used as matrix. It has a reported inherent viscosity of  $0.87 \text{ dL/g}$  measured at a concentration of  $0.5 \text{ g/dL}$  in  $\text{H}_2\text{SO}_4$ . The particulate used in the preparation of composites was  $\text{Al}_2\text{O}_3$  powder of density  $4.00 \text{ g/cm}^3$ . It was used as supplied by Aldrich Chemical Company. Figure 1(a) and (b) are typical SEM micrographs of  $\text{Al}_2\text{O}_3$  and PEEK powder at  $2000\times$  magnification. As received, ethanol of Merck grade was used for homogenizing the  $\text{Al}_2\text{O}_3$  and PEEK mixture. The particle size of the PEEK and  $\text{Al}_2\text{O}_3$  were determined by using GALAI CIS-1 laser particle size analyzer. The particle size of PEEK powder ranges from  $4$  to  $49 \mu\text{m}$  and of  $\text{Al}_2\text{O}_3$  from  $3$  to  $15 \mu\text{m}$ . The mean diameter of the PEEK particle was  $25 \mu\text{m}$  and of the  $\text{Al}_2\text{O}_3$  was  $8 \mu\text{m}$ .



**Scheme 1** Flowchart for preparation of high performance Al<sub>2</sub>O<sub>3</sub>/PEEK composites.

### Sample preparation

Various compositions of composites based on PEEK and Al<sub>2</sub>O<sub>3</sub> were prepared by using the method as reported elsewhere.<sup>25</sup> A brief summary of the process

is shown in a flowchart illustrated in Scheme 1. Dried powder of Al<sub>2</sub>O<sub>3</sub> and PEEK were well premixed through magnetic stirring in alcohol medium for 8 h, and then, the homogeneous slurry was dried in a vacuum oven at 120°C for 10 h and then hot pressed.

A Laboratory hot press was used to fabricate the circular sample of 25 mm diameter in a cylindrical chamber made of tool steel. A mold release agent was used to prevent the PEEK melt from sticking to the die surface. The dried mixed powder of controlled PEEK and Al<sub>2</sub>O<sub>3</sub>/PEEK were filled in a die. Then pressure was applied to compact the powder. The die was heated at an average heating rate of 8°C/min to a maximum temperature of 350°C. The pressure of 15 MPa was kept constant at 350°C for 10 min and then, naturally cooled under pressure below the glass transition temperature of PEEK in a mold at an average cooling rate of 3°C/min. Finally, the samples were ejected out from the mold cavity. The size of molded samples was about 25 mm in diameter and 2 mm in thickness. These samples were polished by using successive emery papers, cleaned with acetone, and dried. Seven different compositions containing 0–50 wt % Al<sub>2</sub>O<sub>3</sub> in PEEK matrix were prepared. Small pieces of composite samples were cut from the compression molded samples for TGA, DSC, and SEM analysis. The actual filler incorporated in the composite samples after processing was determined by TGA (shown in Table I) in air and nitrogen atmosphere.

## CHARACTERIZATION

### Density

Theoretical density of the samples was calculated by rule of mixture (ROM), using the density of Al<sub>2</sub>O<sub>3</sub> 4.00 g/cm<sup>3</sup> and of PEEK 1.29 g/cm<sup>3</sup> for 20% crystalline powder. Experimental density of the filled PEEK samples prepared by hot pressing was measured by Archimedes' principles, where the sample volume is measured by the buoyancy in a immersing medium with known density. The weight and volume is mea-

**TABLE I**  
Actual wt % of Al<sub>2</sub>O<sub>3</sub>, Degradation Temperature (T<sub>10</sub>) of Composites in N<sub>2</sub> and Air at 10 wt % Loss and Char Yield Determined by TGA

Sample code	% Al <sub>2</sub> O <sub>3</sub> in PEEK		Actual wt % of Al <sub>2</sub> O <sub>3</sub> in PEEK determined by TGA		T <sub>d</sub> , air (°C)	T <sub>d</sub> , N <sub>2</sub> (°C)	Char yield % in N <sub>2</sub>
	Wt.	Vol.	In air	In nitrogen			
a	0	0	0	0	556	570	48
b	5	1.67	5.60	5.77	558	564	51
c	10	3.46	8.78	7.69	568	560	52
d	20	7.46	20.00	17.31	566	562	57
e	30	12.14	30.88	28.85	578	572	63
f	40	17.70	37.63	38.46	576	578	68
g	50	24.39	49.00	48.02	582	580	73

sured in air and immersing medium (i.e., alcohol), respectively, at room temperature.

### Thermogravimetric analysis

Actual filler content and thermal stability of the pure PEEK and Al<sub>2</sub>O<sub>3</sub>/PEEK composites were performed on a TGA, using Mettler-Toledo 851e. Approximately 8–10 mg sample was taken in an aluminium pan. The samples were heated from room temperature to 1000°C at the heating rate of 10°C/min in air or nitrogen atmosphere with a flow rate of 50 mL/min. Weight % of char yield was determined by heating samples to 1000°C in a nitrogen atmosphere at a heating rate of 10°C/min.

### Differential scanning calorimetry

Heat of fusion and hot crystallization temperature of PEEK and Al<sub>2</sub>O<sub>3</sub>/PEEK composites were determined by using a Du Pont Instruments 910 DSC. A nitrogen flow rate of 50 mL/min was used. Approximately 20–25 mg samples placed in an aluminum pan were first heated from 30°C to 400°C at a heating rate of 10°C/min and soaked isothermally at 400°C for 5 min to allow complete melting of the polymer. The samples were then cooled to 30°C at a cooling rate of 10°C/min. Each sample was subjected to single heating and cooling cycles under a dry nitrogen purge, and data were recorded during the heating and cooling cycle.

### X-ray diffraction (XRD) measurements

XRD pattern of molded pure PEEK and Al<sub>2</sub>O<sub>3</sub>/PEEK composites was recorded on Philips X'Pert PANalytical PW 3040/60 to qualitatively investigate the development of crystallinity. XRD data were obtained by using CuK $\alpha$  radiation of wavelength 1.54 Å at 40 KV and 30 mA. All the experiments were carried out with 2 $\theta$  varying between 10° and 35° at room temperature.

### Microstructure analysis

A Philips SEM (Philips XL-30) was used to investigate the morphology of pure PEEK and Al<sub>2</sub>O<sub>3</sub>/PEEK composite samples. The distribution of Al<sub>2</sub>O<sub>3</sub> particles in PEEK matrix was also investigated. Small pieces of size about 4 × 4 × 2 mm<sup>3</sup> were cut from the molded sample and mounted in a block of acrylic base polymer resin (DPI-RR cold cure). The obtained sample surfaces were manually ground and polished with successive finer grades of emery papers followed by cloth (mounted on wheel) polishing to remove scratches developed during emery paper polishing. All the samples were rinsed well in water, dried, and

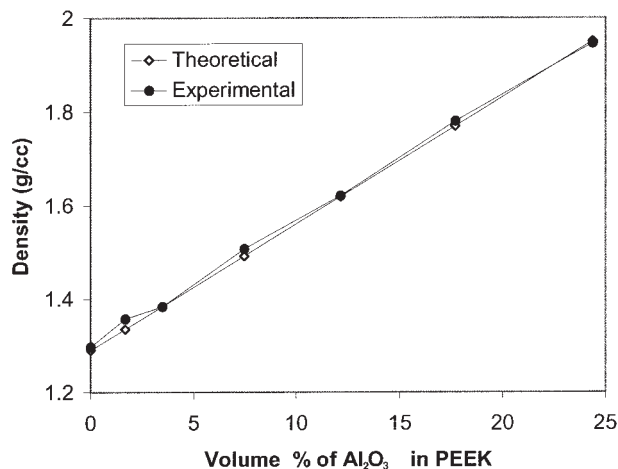


Figure 2 Density of PEEK composites reinforced with Al<sub>2</sub>O<sub>3</sub>.

coated with a thin film of gold before putting into the SEM. The applied voltage was 10–25 KV.

## RESULTS AND DISCUSSION

High performance PEEK composites reinforced with various weight fraction of Al<sub>2</sub>O<sub>3</sub> were prepared by hot pressing technique. Resulting compositions were characterized and discussed in detail in this section. Volume percent of the particles for a given weight fraction can be calculated by using well known eq. (1):

$$V_f = W_f / [W_f + (1 - W_f) \cdot \rho_f / \rho_m] \quad (1)$$

where  $V_f$  is the volume fraction,  $W_f$  is the weight fraction,  $\rho_f$  is the density of Al<sub>2</sub>O<sub>3</sub> particles, and  $\rho_m$  is the density of the polymer matrix.

### Density

Figure 2 showed the density of the Al<sub>2</sub>O<sub>3</sub>-filled PEEK as a function of Al<sub>2</sub>O<sub>3</sub> content. It can be seen that the density increased with Al<sub>2</sub>O<sub>3</sub> loading in a linear fashion. The experimental density of the composites except composite (g) is more than the theoretical density. In another study on a different composite system, a similar observation was reported.<sup>22</sup> However, in hydroxyapatite (HA)-reinforced PEEK composites, the experimental density is equal or less than the theoretical density. In present study, higher density might be an indication of the porosity free samples due to good processing conditions and increased crystallinity as a result of the nucleation effect of Al<sub>2</sub>O<sub>3</sub> particles.

### Thermogravimetric analysis

TGA measurement was carried out to obtain actual incorporated filler and thermal stability of the pure

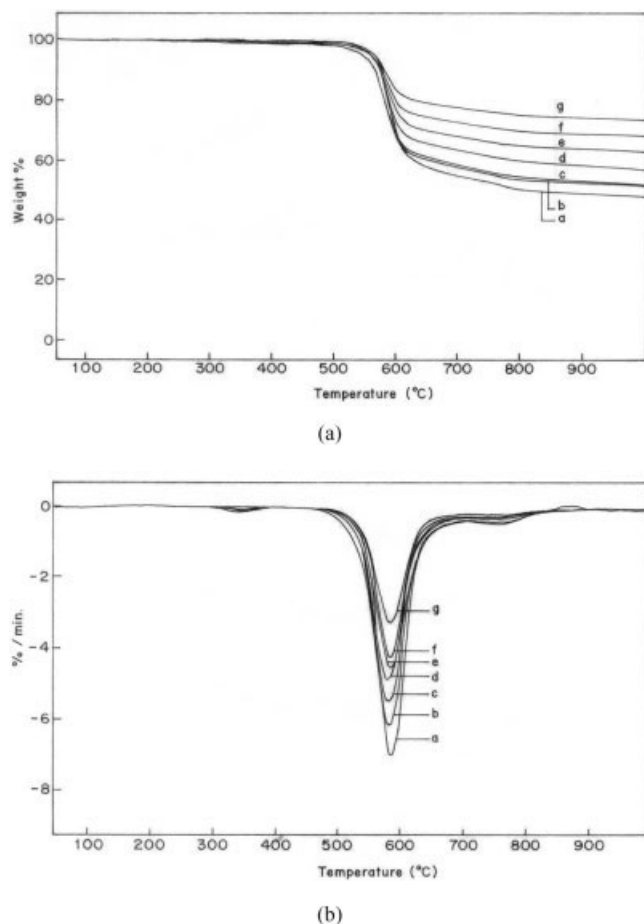


**Figure 3** (a) TGA curves of PEEK composites (a–g) in nitrogen atmosphere; (b) DTG curves of PEEK composites (a–g) in nitrogen atmosphere.

PEEK and Al<sub>2</sub>O<sub>3</sub>/PEEK composites. The percentage of original weight remaining as a function of the temperature under nitrogen and air atmosphere was shown in Figures 3(a) and 4(a), respectively. The temperature at 10 wt % loss was taken as the degradation temperature ( $T_{10}$ ) and tabulated in Table I. It can be seen from the Table I that pure PEEK has  $T_{10}$  in nitrogen atmosphere ( $T_{10, N_2}$ ) at 570°C. It is observed that as the percentage of Al<sub>2</sub>O<sub>3</sub> increases in PEEK the thermal stability of composites in nitrogen atmosphere is decreased up to 20 wt %, but afterwards increased to 580°C for PEEK with 50 wt % Al<sub>2</sub>O<sub>3</sub>. However, the thermal stability of composites in air atmosphere is increased for all compositions, i.e., by 26°C from 556°C for the pure PEEK to 582°C for PEEK with 50 wt % Al<sub>2</sub>O<sub>3</sub>. Therefore, the incorporation of Al<sub>2</sub>O<sub>3</sub> in PEEK matrix improved thermal stability of the composites. The increase in thermal stability could be due to strong interaction or interfacial bonding between the polymer matrix and the Al<sub>2</sub>O<sub>3</sub> particles.

Figures 3(b) and 4(b) showed the derivative thermogravimetric analysis curves of composites in nitrogen and air atmosphere, respectively. It can be seen from

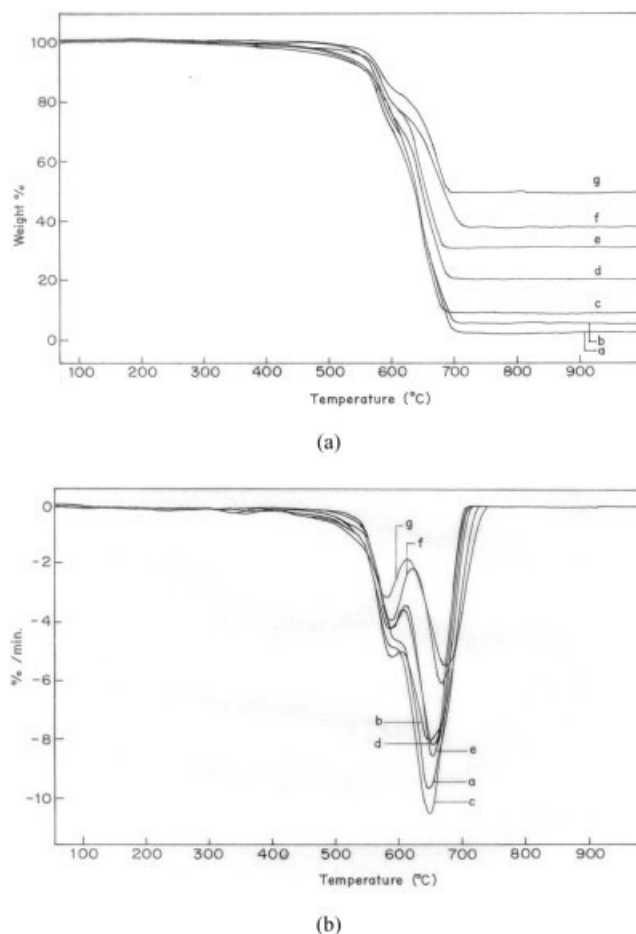


**Figure 4** (a) TGA curves of PEEK composites (a–g) in air atmosphere; (b) DTG curves of PEEK composites (a–g) in air atmosphere.

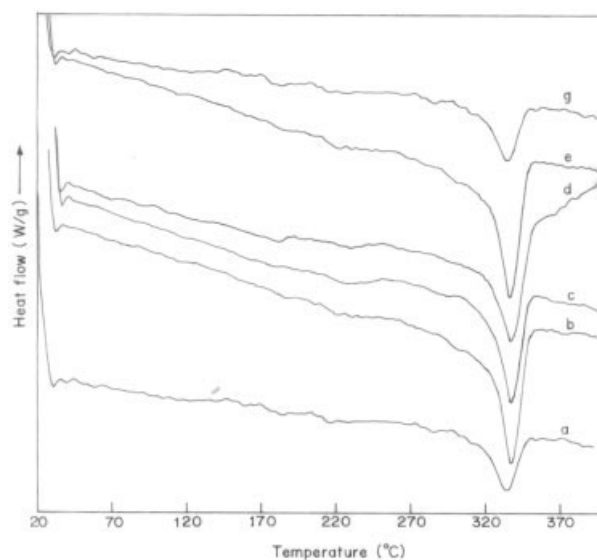


**Figure 5** DSC heating curves of PEEK composites (a–g).

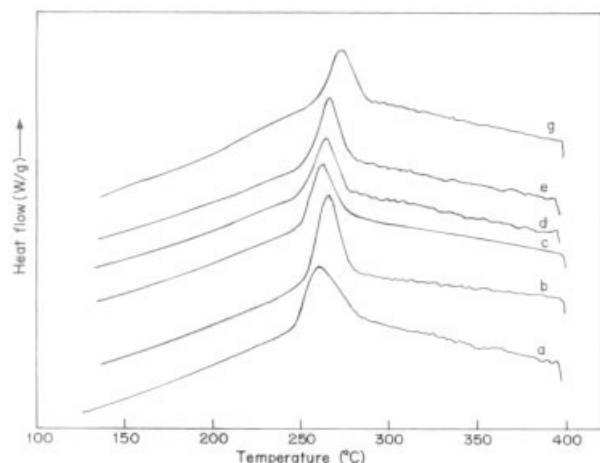


Figure 6 DSC cooling curves of PEEK composites (a–g).

Figure 3(b) that there is not any change in maximum decomposition temperature in nitrogen atmosphere for all composite samples. However, the decomposition temperature range is decreased as the wt % of  $\text{Al}_2\text{O}_3$  content increased. Figure 4(b) showed two decomposition stages of PEEK composites under air atmosphere in contrast to single decomposition stage under nitrogen atmosphere. In air atmosphere also there is not any significant change in maximum decomposition temperature except composite (f).

The actual incorporated wt % of  $\text{Al}_2\text{O}_3$  in PEEK matrix was determined by heating the sample to  $1000^\circ\text{C}$  in air atmosphere. It can be seen from the Figure 4(a) that pure PEEK showed negligible residue at  $1000^\circ\text{C}$  in air. Therefore, the residue of the composites remained at  $1000^\circ\text{C}$  in TGA analysis would be the wt % of the  $\text{Al}_2\text{O}_3$  in PEEK matrix as summarized in Table I. Moreover, the actual incorporated wt % of  $\text{Al}_2\text{O}_3$  in PEEK matrix was also determined in nitrogen atmosphere by assuming that  $\text{Al}_2\text{O}_3$  does not affect the degradation rate of PEEK matrix in composites. Therefore, the wt % of the degraded PEEK matrix i.e., char yield of pure PEEK may be taken as constant in all compositions. The actual incorporated wt % of  $\text{Al}_2\text{O}_3$  in PEEK matrix in nitrogen atmosphere was determined by using the mass balance eq. (2) and the results are summarized in Table I.

TABLE II  
Thermal Properties of Composites During Heating Cycle

Sample code	$T_m$ ( $^\circ\text{C}$ )	$\Delta H_f$ (J/g)	$\Delta H_f$ (J/g) <sup>a</sup>	% $\chi_{c,DSC}$
a	333.74	26.07	26.07	20.05
b	336.67	40.90	43.05	33.12
c	337.04	28.14	31.27	24.05
d	338.02	39.34	49.18	37.83
e	336.69	21.24	30.34	23.34
g	336.11	16.33	32.66	25.12

<sup>a</sup> Normalized heat of fusion of PEEK constituent in  $\text{Al}_2\text{O}_3/\text{PEEK}$  composite.

$$W_f = [(W_c - W_m)/(1 - W_m/100)] \quad (2)$$

where  $W_f$  is the wt % of  $\text{Al}_2\text{O}_3$  in PEEK matrix,  $W_c$  is the wt % char yield of composite, and  $W_m$  is the wt % char yield of pure PEEK in nitrogen atmosphere.

As shown in Table I, there is some difference in theoretical and actual wt % of  $\text{Al}_2\text{O}_3$  in PEEK matrix. This might be due to two reasons. First, because of the loss of a little quantity of  $\text{Al}_2\text{O}_3$  or PEEK powder during the composites mixing process due to difference in density of components. Second, because of the desorption of physisorbed water and dehydration of  $\text{Al}_2\text{O}_3$ .<sup>26</sup>

It can be seen from the Table I that the char yield of pure PEEK is about 48%, in agreement with a reported value.<sup>27</sup> The char yield was increased from 48% for the pure PEEK to 73% for PEEK reinforced with 50 wt %  $\text{Al}_2\text{O}_3$ . It is well known that  $\text{Al}_2\text{O}_3$  is thermally most stable at higher temperature. Hence, the increase in char yield is due to the increase in wt % of  $\text{Al}_2\text{O}_3$  in composites.

### Differential scanning calorimetry

DSC measurements were carried out to determine the percentage crystallinity, heat of fusion, and crystallization temperature of PEEK and  $\text{Al}_2\text{O}_3/\text{PEEK}$  composites. The DSC heating and cooling curves are shown in Figures 5 and 6 for PEEK composite, respectively. From the recorded heating and cooling curves, thermal properties such as melting temperature ( $T_m$ ), onset temperature to recrystallization ( $T_{on}$ ), peak crys-

TABLE III  
Thermal Properties of Composites During Cooling Cycles

Sample code	$T_c$ ( $^\circ\text{C}$ )	$T_{on}$ ( $^\circ\text{C}$ )	$\Delta H_c$ (J/g)	$\Delta H_c$ (J/g) <sup>a</sup>	% $\chi_{c,DSC}$	$t_{1/2}$ (min)	$\Delta T$ ( $^\circ\text{C}$ )
a	259.65	280.11	39.76	39.76	30.58	2.05	74
b	264.33	276.86	44.60	46.95	36.12	1.25	72
c	261.57	274.30	37.93	42.14	32.42	1.27	75
d	265.53	276.65	31.44	38.93	29.90	1.11	73
e	268.48	279.32	29.98	37.48	28.83	1.08	68
g	272.40	284.51	26.15	52.30	40.23	1.21	64

<sup>a</sup> Normalized heat of crystallization of PEEK constituent in  $\text{Al}_2\text{O}_3/\text{PEEK}$  composite.

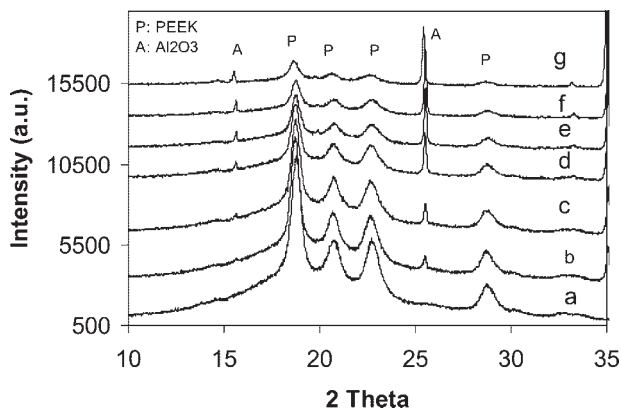


**Figure 7** XRD Pattern of PEEK composites (a–g), for clarity, scans for sample (b–g) has been displaced upward.

tallization temperature ( $T_c$ ), heat of crystallization ( $H_c$ ), heat of fusion ( $H_m$ ), and degree of crystallinity were calculated and tabulated in Tables II and III. Degree of crystallinity ( $\chi_{c, disc}$ ) were obtained by using the method described elsewhere.<sup>25</sup>

It is seen from the curves (a–g) of Figure 5 that the  $T_m$  is increased by 2–4°C as the  $Al_2O_3$  loading increases in PEEK. However, in our earlier study, we observed 11°C increase in  $T_m$  for PEEK reinforced with 50 wt % AlN.<sup>25</sup> In another composite system, a decrease in  $T_m$  by 5°C from 338°C for pure PEEK to 333°C for PEEK reinforced with 30 wt % sulfonated PEEK (SPEEK)-treated  $CaCO_3$  of 80 nm particle sized was observed. For the same composition 6°C decrease in  $T_m$  was observed when untreated  $CaCO_3$  was used.<sup>28</sup> However, a decrease in  $T_m$  about 13°C was observed from 338°C for pure PEEK to 325°C for PEEK reinforced with 30 wt % SPEEK-treated  $CaCO_3$  of 2  $\mu m$  sized. Pingping et al. have reported that in  $CaCO_3$ /PET composites the addition of  $CaCO_3$  particles does not have significant effect on  $T_m$  of composites.<sup>29</sup> Thus, we believe that the increase in  $T_m$  in our both the cases may results from the well-dispersed particles that increase the crystallinity of the PEEK as confirmed by density, DSC, and XRD. Therefore, particle size and method of mixing of the filler particles

and polymer has important role in changing the  $T_m$  of composites whereas surface treatment of fillers has negligible role.

During cooling cycle, it was observed that the  $T_{on}$ ,  $T_c$  and half-time of crystallization ( $t_{1/2}$ ) of PEEK was affected by the presence of the  $Al_2O_3$ , which indicate that nucleation is inhomogeneous. It can be seen from the curves (a–g) of Figure 6, that addition of  $Al_2O_3$  content in PEEK shifts the peak crystallization temperature ( $T_c$ ) by 12°C for a given cooling rate in comparison to pure PEEK, indicating that the addition of  $Al_2O_3$  into PEEK enhanced the rate of PEEK crystallization.<sup>30,31</sup> This result is in contrast to the untreated and SPEEK-treated  $CaCO_3$  dispersed PEEK, where  $CaCO_3$  do not act as nucleating agents, evidenced by a significant increase in time to reach the exothermic peak.<sup>28</sup>

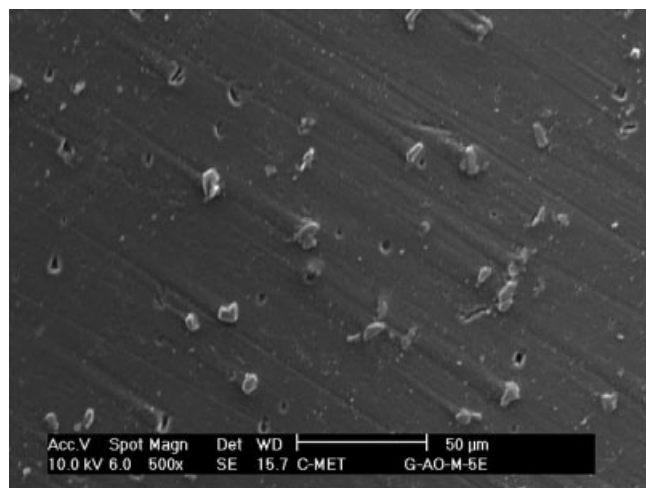
The half-time ( $t_{1/2}$ ) of crystallization temperature of pure PEEK and  $Al_2O_3$ /PEEK was determined by using the equation [ $t_{1/2} = (T_{on} - T_c)/\text{rate of cooling}$ ]. Table III showed that  $t_{1/2}$  value of composite decreases with the increase in  $Al_2O_3$  content in pure PEEK. These results are similar to the  $CaCO_3$ /PP system where  $CaCO_3$  particles of 6  $\mu m$  reduced the crystallization half-time significantly.<sup>32</sup> The  $t_{1/2}$  for the pure PEEK 2.05 min is reduced to 1.08 min for the PEEK with 40 wt %  $Al_2O_3$ . Thus,  $Al_2O_3$  particles accelerate the crystallization process of pure PEEK. For the same rate of cooling, there is enough time for the molecular chains of PEEK to pack into a closer arrangement.

#### X-ray diffraction measurements

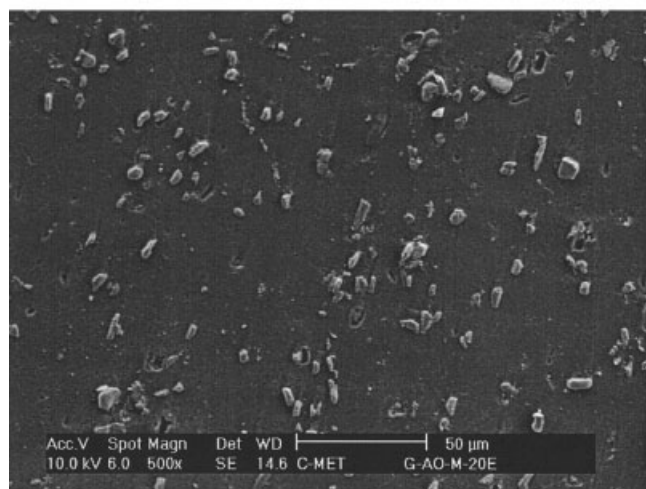
The angular position in the range of  $2\theta = 10^\circ$ – $35^\circ$  of major crystallographic reflection for the PEEK and  $Al_2O_3$ /PEEK composite sample are shown in Figure 7. XRD pattern in Figure 7 showed that pure PEEK and its composites crystallizes primarily in the orthorhombic form showing diffraction peaks corresponding to Miller indices, (110), (111), (200), and (211) Here, we have shown only two diffraction peaks of  $Al_2O_3$  at 15.66 and 25.57°.

**TABLE IV**  
Angular Position and Inter-Planer Distance of Composites Determined by XRD

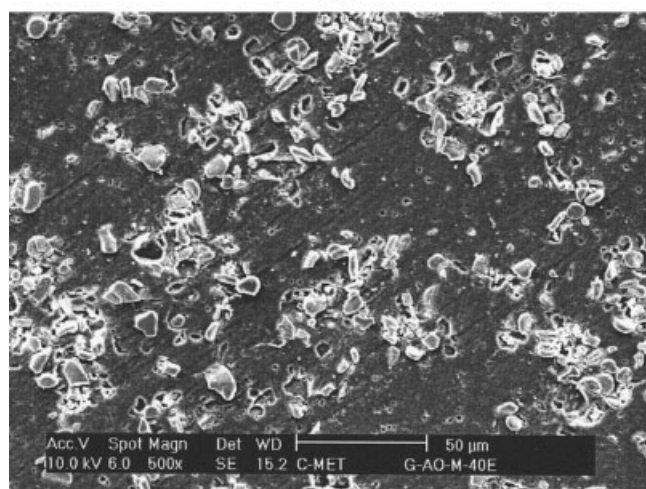
Sample code	$2\theta$ (°)				Inter planer spacing $d_{hkl}$ (nm)			
	$2\theta_{110}$	$2\theta_{111}$	$2\theta_{200}$	$2\theta_{211}$	$d_{110}$	$d_{111}$	$d_{200}$	$d_{211}$
a	18.525	20.564	22.573	28.489	0.4790	0.4319	0.3939	0.3133
b	18.777	20.536	22.536	28.633	0.4722	0.4288	0.3942	0.3115
c	18.699	20.736	22.591	28.599	0.4742	0.4280	0.3933	0.3119
d	18.773	20.657	22.756	28.746	0.4707	0.4296	0.3905	0.3103
e	18.794	20.782	22.723	28.766	0.4718	0.4271	0.3910	0.3101
f	18.745	20.788	22.672	28.729	0.4730	0.4270	0.3919	0.3105
g	18.630	20.621	22.792	28.566	0.4759	0.4304	0.3899	0.3122



(a)



(b)



(c)

**Figure 8** SEM micrograph of polished and etched sample of (a) sample b, (b) sample d, and (c) sample f.

It can be seen from the Table IV that there is a displacement of reflection toward a higher angular position when compared with pure PEEK with increasing  $\text{Al}_2\text{O}_3$  content. The inter planer spacing,  $d_{hkl}$  of different crystalline planes ( $hkl = 110, 111, 200, 211$ ) are the highest for the pure PEEK, but decreases as the  $\text{Al}_2\text{O}_3$  content increases in PEEK. A smaller  $d_{hkl}$  for composite may be attributed to perfection of crystals. A remarkable decrease in  $d_{110}$ ,  $d_{111}$ ,  $d_{200}$ , and  $d_{211}$  were observed in direction perpendicular to plane, (110), (111), (200), and (211), respectively. Table IV showed total decrease in  $d_{hkl}$  of about 0.08, 0.05, 0.04 and 0.02 Å for the (110), (111), (200), and (211) planes, respectively. Because of the decrease of  $d$ -spacing, the dimensions of crystalline units decreases as the  $\text{Al}_2\text{O}_3$  content increases and thus, improve the crystallinity of bulk composite. This type of effect was reported for the pure PEEK as the annealing time or temperature of crystallization was increased.<sup>33</sup> The quantitative increase in crystallinity was confirmed by dsc technique.

### Scanning electron microscope

The morphological and particles distribution in polymer matrix was studied using SEM. Figure 1(a) and (b) showed micrographs of  $\text{Al}_2\text{O}_3$  and pure PEEK powder at 2000× magnification.  $\text{Al}_2\text{O}_3$  particles have a flat platelet of size ranging from 3 to 15  $\mu\text{m}$ . PEEK powders have irregular particles of rod-like shape of length ranging from 10 to 50  $\mu\text{m}$ . Figure 8(a)–(c) showed the SEM of polished and etched composites of PEEK reinforced with 5, 20, and 40 wt %  $\text{Al}_2\text{O}_3$ , respectively. The polished samples were etched for 20 min, using a 2% w/v solution of potassium permanganate in a mixture of 4 volumes of *o*-phosphoric acid and 1 volume of water. The  $\text{Al}_2\text{O}_3$  particles were uniformly dispersed in all composite samples. There were no aggregates of  $\text{Al}_2\text{O}_3$  particles in PEEK matrix, which is expected due to good processing condition during the sample preparation.

### CONCLUSIONS

Dense and homogeneous high performance PEEK matrix composites incorporating  $\text{Al}_2\text{O}_3$  up to 50 wt % were prepared by mixing PEEK and  $\text{Al}_2\text{O}_3$  powders in alcohol medium followed by hot pressing technique. The thermal stability of composites in air atmosphere was higher than in nitrogen atmosphere. The improvement in thermal stability of the composites could be due to strong interaction or interfacial bonding between the PEEK matrix and the  $\text{Al}_2\text{O}_3$  particles. The peak crystallization temperature and crystallinity of the composites was increased because of strong nucleating effect of  $\text{Al}_2\text{O}_3$ . Hence, half-time of crystallization is reduced considerably.



The authors thank Dr. P. D. Trivedi, Polymer Division, Gharda Chemicals, India for providing good quality PEEK powder for this research work. We would also acknowledge Dr. S. L. Kamath, IIT, Bombay, for performing DSC analysis, Dr. D. P. Amalnerkar/Mrs V. D. Giramkar, C-MET, for SEM analysis, and Dr. U. P. Mulik/Mrs. Shany Joseph, C-MET, for TGA analysis. R. K. Goyal gratefully acknowledges to the executive director of C-MET.

## References

1. Melo, J. D. D.; Radford, D. W. *Compos A* 2002, 33, 1505.
2. Wong, C. P.; Raja, S. B. *J Appl Polym Sci* 1999, 74, 3396.
3. Nakamura, Y.; Yamahuchi, M.; Okubo, M.; Matsumoto, T. *J Appl Polym Sci* 1992, 44, 151.
4. Bhattacharya, S. K.; Tummala, R. R. *Microelectronics J* 2001, 32, 11.
5. Xu, Y.; Chung, D. D. L.; Mroz, C. *Compos A* 2001, 32, 1749.
6. Suwanprateeb, J. *Compos A* 2000, 31, 353.
7. Chan, C. M.; Wu, J.; Li, J.-X.; Cheung, Y.-K. *Polymer* 2002, 43, 2981.
8. Cheng, S. Z. D.; Cao, M.-Y.; Wunderlich, B. *Macromolecules* 1986, 19, 1868.
9. Huo, P.; Cebe, P. *Macromolecules* 1992, 25, 902.
10. Kalika, D. S.; Krishnaswami, R. K. *Macromolecules* 1993, 26, 4252.
11. Krishnaswami, R. K.; Kalika, D. S. *Polymer* 1994, 35, 1157.
12. Jonas, A.; Legras, R. *Macromolecules* 1993, 26, 813.
13. Bas, C.; Battesti, P.; Alberola, N. D. *J Appl Polym Sci* 1994, 53, 1745.
14. Lee, Y.; Porter, R. S.; Lin, J. S. *Macromolecules* 1989, 22, 1756.
15. Atkinson, J. R.; Hay, J. N.; Jenkins, M. J. *Polymer* 2002, 43, 731.
16. Attwood, T. E.; Dawson, P. C.; Freeman, J. L.; Hoy, L. R. J.; Rose, J. B.; Staniland, P. A. *Polymer* 1981, 22, 1096.
17. Blundell, D. J.; Osborn, B. N. *Polymer* 1983, 24, 953.
18. Wang, Q. H.; Xu, J.; Shen, W.; Xue, Q. *Wear* 1997, 209, 316.
19. Wang, Q.; Xue, Q.; Shen, W. *Tribol Int* 1997, 30, 193.
20. Wang, Q. H.; Xu, J.; Shen, W.; Liu, W. *Wear* 1996, 196, 82.
21. Wang, Q. H.; Xu, J.; Liu, H.; Shen, W.; Xu, J. *Wear* 1996, 198, 216.
22. Baker, M. S. A.; Cheang, P.; Khor, K. A. *J Mater Process Tech* 1999, 89/90, 462.
23. Kuo, M. C.; Tsai, C. M.; Huang, J. C.; Chen, M. *Mater Chem Phys* 2005, 90, 185.
24. Sandler, J.; Werner, P.; Sheffer, M. S. P.; Demchuk, V.; Altstädt, V.; Windle, A. H. *Compos A* 2002, 33, 1033.
25. Goyal, R. K.; Tiwari, A. N.; Negi, Y. S. *Eur Polym J* 2005, 41, 2034.
26. Abboud, M.; Turner, M.; Duguet, E.; Fontanille, M. *J Mater Chem* 1997, 7, 1527.
27. Roovers, J.; Cooney, J. D.; Toporowski, P. M. *Macromolecules* 1990, 23, 1611.
28. Tang, J.; Wang, Y.; Liu, H.; Belfiore, L. A. *Polymer* 2004, 45, 2081.
29. Gutzow, D. J. I. *J Non-Cryst Solids* 1993, 162, 13.
30. Zhou, B.; Ji, X.; Sheng, Y.; Wang, L.; Jiang, Z. *Eur Polym J* 2004, 40, 2357.
31. Pingping, Z.; Dezh, M. *Eur Polym J* 2000, 36, 2471.
32. Khare, A.; Mitra, A.; Radhakrishnan, S. *J Mater Sci* 1996, 31, 5691.
33. Hay, J. N.; Langford J. I.; Lloyd, J. R. *Polymer* 1989, 30, 489.